

M. TULIŃSKI\*, M. JURCZYK\*

## MECHANICAL AND CORROSION PROPERTIES OF NI-FREE AUSTENITIC STAINLESS STEELS

### ODPORNOŚĆ KOROZYJNA I WŁAŚCIWOŚCI MECHANICZNE BEZNIKLOWYCH AUSTENITYCZNYCH STALI NIEDZEWNYCH

In the presented work Ni-free austenitic stainless steels with nanostructure were synthesized by mechanical alloying (MA), heat treatment and nitrogenation of elemental microcrystalline Fe, Cr, Mn and Mo powders. Phase transformation from ferritic to austenitic was confirmed by XRD analysis. The mechanical properties of produced biomaterials were investigated using Vickers and nanoindentation methods. Corrosion tests were performed in H<sub>2</sub>SO<sub>4</sub> and Ringer's solution. An enhancement of properties due to the nanoscale structures in bulk consolidated materials has been observed.

*Keywords:* nickel-free stainless steel, mechanical alloying, biomaterials

W niniejszej pracy badano beznikłowe austenityczne stale nierdzewne z nanostrukturą otrzymane za pomocą mechanicznej syntezy, obróbki cieplnej i azotowaniu wyjściowych proszków Fe, Cr, Mn i Mo. Przemiana fazowa z ferrytycznej w austenityczną została potwierdzona badaniami rentgenowskimi. Właściwości mechaniczne otrzymanych materiałów były badane metodą Vickers'a oraz za pomocą nanoindentera. Odporność korozyjna była badana w środowisku H<sub>2</sub>SO<sub>4</sub> oraz płynu Ringera. Zaobserwowano poprawę właściwości dla otrzymanych materiałów, związaną z otrzymaniem nanostruktury.

## 1. Introduction

Mechanical and corrosion resistance properties of typical metallic biomaterials used for implant devices are relatively good and satisfactory but these materials may also cause many problems within human body and therefore need improvement. The main disadvantage of the most popular austenitic stainless steel (316L) [1] is lack of biocompatibility, toxicity of corrosion products and fracture due to corrosion fatigue [2]. Austenite stabilizer – nickel – is reported to be an especially toxic element which causes allergies and even cancer [3]. World Health Organization (WHO) estimated that content of less than 0.2% of nickel is congruous with medical requirements [2]. Therefore development of materials with either improved corrosion resistance and without nickel content is absolutely imperative.

One of the most promising austenitizing elements to replace nickel is nitrogen [4]. Nitrogen increases austenite stability, corrosion resistance and prevents from the formation of sigma phase.

Recently, a new manufacturing process of nickel-free austenitic stainless steels with nitrogen ab-

sorption treatment has been developed [5]. In this method, small devices can be precisely machined in a ferritic phase and than during nitrogenation of their surfaces in nitrogen gas at temperature approx. 1200°C they become nickel-free austenitic stainless steels with better mechanical and corrosion resistance properties.

In this work, a new manufacturing process of nickel-free austenitic stainless steels with nanostructure has been proposed. Ni-free austenitic stainless steels with nanostructure were synthesized by mechanical alloying (MA), heat treatment and nitrogenation of elemental microcrystalline Fe, Cr, Mn and Mo powders.

Mechanical alloying (MA) was developed in the 1970's at the International Nickel Co. as a technique for dispersing nanosized inclusions into nickel-based alloys [6]. During the last years, the MA process has been successfully used to prepare a variety of alloy powders including powders exhibiting supersaturated solid solutions, quasicrystals, amorphous phases and nano-intermetallic compounds. MA technique has been proven a novel and promising method for alloy formation.

\* INSTITUTE OF MATERIALS SCIENCE AND ENGINEERING POZNAŃ UNIVERSITY OF TECHNOLOGY, MARIII SKŁODOWSKIEJ-CURIE SQ 5, 60-965 POZNAŃ, POLAND

The raw materials used for MA are commercially available as high purity powders that have sizes in the range of 1-100  $\mu\text{m}$ . During the mechanical alloying process, the powder particles are periodically trapped between colliding balls and are plastically deformed. Such a feature occurs by the generation of a wide number of dislocations as well as other lattice defects. Furthermore, the ball collisions cause fracturing and cold welding of the elementary particles, forming clean interfaces at the atomic scale. Further milling leads to increase of the interface number and the sizes of the elementary component area decrease from millimeter to submicrometer lengths. Concurrently to this decrease of the elementary distribution, some nanocrystalline intermediate phases are produced inside the particles or at its surfaces. As the milling duration develops, the content fraction of such intermediate compounds increases leading to a final product which properties are the function of the milling conditions.

Details of the process and the enhancement of prop-

erties due to obtaining nanostructure in consolidated materials are presented.

## 2. Experimental

The FeCrMnMoN alloys were prepared by mechanical alloying of stoichiometric amounts of the constituent elements (99.9% or better purity). Mechanical alloying was carried out using a SPEX 8000 Mixer Mill fitted with a hardened steel vial and 10 mm diameter steel balls. The vial of the SPEX Mill was loaded with powder in a glove-box connected to a high purity argon supply. The elemental powders (Fe: 10  $\mu\text{m}$ , Cr: 5  $\mu\text{m}$ , Mn: 44  $\mu\text{m}$ , Mo: 10  $\mu\text{m}$ ) were mixed and poured into the vial (Fig. 1a). The mill was run up to 48 h for every powder preparation (Fig. 1b). The as-milled powders were heat treated at 750°C for 0.5 h, under high purity argon, to form ordered phases (Fig. 1c). Nitrogenation of cold pressed samples was carried out at temperature 1210°C for 24 hours at 140 kPa nitrogen pressure (Fig. 1e).

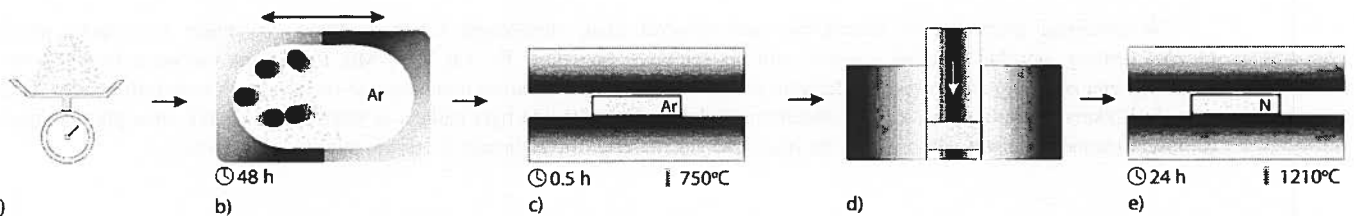


Fig. 1. Schematic representation of experimental process of manufacturing of nanocrystalline stainless steels: (a) initial powders, (b) mechanical alloying, (c) heat treatment, (d) cold pressing, (e) nitrogen absorption

The powders were characterized by means of X-ray diffraction (XRD). XRD was performed using an X-ray powder diffractometer with Co  $K\alpha$  radiation, at various stages during milling, prior to annealing and after annealing as well as after nitrogenation.

Microhardness measurements were carried out in Vickers method with the load of 200g. The micrographs were obtained using an optical microscope. The density of the sintered samples was determined by the Archimedes method. For selected samples nanoindentation test was done.

Embrittlement and related to it stress intensity factor –  $K_{Ic}$  – was investigated using Vickers method with the load of 200 g, 500 g, 1 kg, 2 kg, 5 kg, 10 kg and 30 kg.

The analyses of the corrosion were conducted on a Solartron 1285 potentiostat in Princeton Applied Research corrosion cell system. This system was interfaced to a personal computer. The experiments were controlled and the data were analyzed using a CorrWare analysis software. Counter electrodes are graphite and the reference electrode is SCE ( $\text{Hg}/\text{Hg}_2\text{Cl}_2 - \text{Sat. KCl}$ ). The

method of polarization resistance was employed to investigate the change in corrosion. The etching solution was 0.1 M  $\text{H}_2\text{SO}_4$  and Ringer's solution (sodium chloride 9.00 g/l, potassium chloride 0.42 g/l, calcium chloride 0.48 g/l, sodium hydrogen carbonate 0.20 g/l). Scanning range and speed were -1 to 2.5 V and 0.5 mV/s, respectively. Experiments were carried out at 25°C in case of  $\text{H}_2\text{SO}_4$  and 37°C in case of Ringer's solution. From the analyses, the corrosion current,  $I_{\text{corr}}$ , were recorded. The corrosion rate (mmPY) can be then calculated, using CorrWare software, by as follows:

$$\text{Corrosion rate} = 0.00408 I_{\text{corr}} A / n D \quad (1)$$

where  $I_{\text{corr}}$  is the corrosion current ( $\text{A}/\text{cm}^2$ ),  $D$  is the density and  $A/n$  is the effective weight.

The value  $D$  for stainless steel was 7.8  $\text{g}/\text{cm}^3$ . The value of the effective weight,  $A/n$ , was 25.29 g.

The steel specimens were in the form of rods. The specimens were prepared and mounted according to the following steps. The stainless steel rods were formed in

the dimensions of 8 mm diameter and 3 mm long. A stainless steel rod 200 mm long and 3.5 mm diameter was used for establishing the electrical contact. The whole assembly was inserted in a glass tube. Silicon resin was used to ensure the exposure of a determined apparent surface area of  $0.5 \text{ cm}^2$ .

### 3. Results and discussion

The effect of MA processing was studied by X-ray diffraction and microstructural investigations. In this

work Ni-free austenitic stainless steels with nanostructure were synthesized by mechanical alloying (MA), heat treatment and nitrogenation of elemental microcrystalline Fe, Cr, Mn and Mo powders. After 48 h of MA the alloy had decomposed into an amorphous phase and nanocrystalline  $\alpha$ -Fe [7]. Heat treatment performed after MA process results in crystallization into ferritic phase. Then, compacted material was nitrided at  $1210^\circ\text{C}$  which resulted in phase transformation from ferritic to fully austenitic (Fig. 2) [8]. Crystallite size of so produced material, 27 nm, was estimated by Scherrer's method.

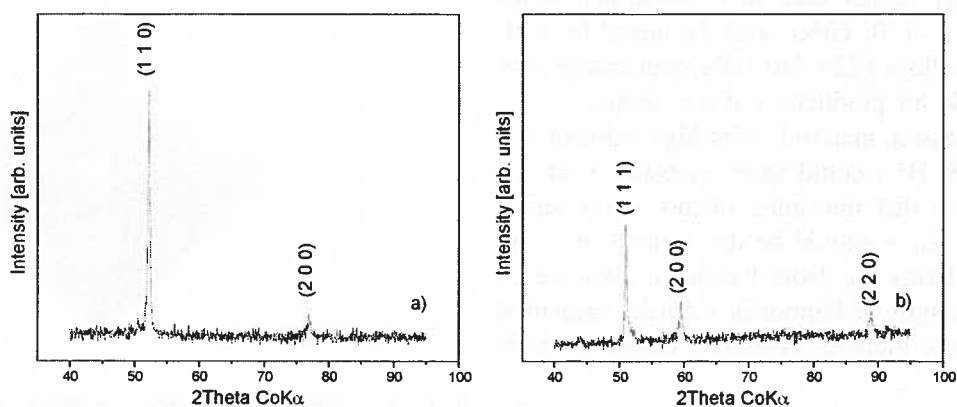


Fig. 2. Phase transformation from ferritic (a) to austenitic (b)

The microhardness of the final bulk material was studied using Vickers method and the results are presented on Fig. 3. Compared with widely used in medicine 316L stainless steel (248 HV0.2), microhardness of sintered nanocrystalline austenitic nickel-free nitrogen con-

taining stainless steels obtained by mechanical alloying is significantly higher (378 to 520 HV0.2). The result is two times greater than in austenitic steel obtained by conventional methods. This effect is directly connected with structure refinement and obtaining of nanostructure.

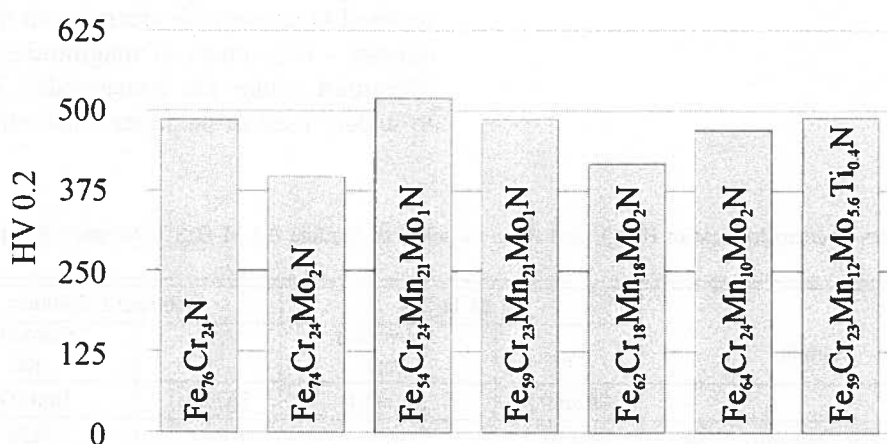


Fig. 3. Microhardness of produced FeCrMnMoN materials

The microhardness and Young's modulus of selected samples of Ni-free stainless steels with nanostructure was studied using nanoindenter. Results are presented in Table 1. They are comparable with results of Vickers

test. Microhardness remains on the level of 500 HV in case of Ni-free stainless steels with nanostructure and 276 HV for 316L stainless steel.

TABLE 1

Results of microhardness and Young's modulus tests for selected samples of Ni-free austenitic stainless steels and 316L stainless steel

Sample	HV	H (MPa)	E (GPa)
316L	276	2977	172
Fe <sub>74</sub> Cr <sub>24</sub> Mo <sub>2</sub> N	650	7014	201
Fe <sub>54</sub> Cr <sub>24</sub> Mn <sub>21</sub> Mo <sub>1</sub> N	542	5846	210
Fe <sub>59</sub> Cr <sub>23</sub> Mn <sub>12</sub> Mo <sub>6</sub> N	525	5663	213
Fe <sub>64</sub> Cr <sub>24</sub> Mn <sub>10</sub> Mo <sub>2</sub> N	469	5027	199

Young's modulus of obtained steels is about 210 GPa that is slightly higher than in conventional stainless steel 316L (~170 GPa) and comparable with cobalt-chromium alloys (220-240 GPa) that makes this material applicable for production of e.g. stents.

As one may expect, materials with high value of microhardness (~500 HV) could show embrittlement. To exclude or endorse that unwanted phenomenon, stress intensity factor –  $K_{Ic}$  – should be determined. It could be done by calculating  $K_{Ic}$  from hardness, diameter of indentation and length of Palmquist's cracks measured directly in Vicker's method. Niihara's equation apply here [9].

Imprint of Vicker's indenter (for clarity – only for 30kg load) on polished surface of Ni-free stainless steel with nanostructure (Fe<sub>59</sub>Cr<sub>23</sub>Mn<sub>12</sub>Mo<sub>6</sub>N) is shown on the Figure 4. Load of 200 g, 500 g, 1 kg, 2 kg, 5 kg, 10 kg and even 30 kg did not reveal any marks of Palmquist's cracks.

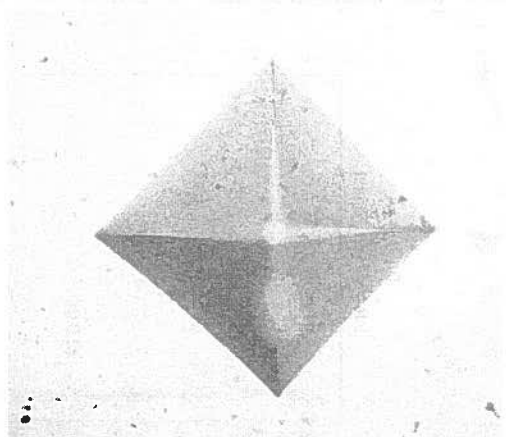


Fig. 4. Imprint of Vicker's indenter (30 kg load) for Fe<sub>59</sub>Cr<sub>23</sub>Mn<sub>12</sub>Mo<sub>6</sub>N sample

Table 2 summarizes results of corrosion tests in H<sub>2</sub>SO<sub>4</sub> and Ringer's solution. In H<sub>2</sub>SO<sub>4</sub> the corrosion current,  $I_{corr}$ , in the case of Fe<sub>59</sub>Cr<sub>23</sub>Mn<sub>12</sub>Mo<sub>6</sub>N is  $1.3 \times 10^{-5}$  A/cm<sup>2</sup>. The corresponding values of Fe<sub>54</sub>Cr<sub>24</sub>Mn<sub>21</sub>Mo<sub>1</sub>N and Fe<sub>64</sub>Cr<sub>24</sub>Mn<sub>10</sub>Mo<sub>2</sub>N are  $1.6 \times 10^{-4}$  and  $5.14 \times 10^{-4}$  A/cm<sup>2</sup>, respectively.  $I_{corr}$  values indicate that addition of Mo and reduction of Mn resulted in appreciable decrease in the corrosion current density – two orders of magnitudes and corrosion rate. Measured values are considerably improved compared to widely used in medicine 316L stainless steel.

TABLE 2

Results of corrosion test in H<sub>2</sub>SO<sub>4</sub> and Ringer's solution. Sample 0.1 M H<sub>2</sub>SO<sub>4</sub> Ringer's Solution

Sample	0.1 M H <sub>2</sub> SO <sub>4</sub>		Rinnger's Solution	
	$I_{corr}$ [A/cm <sup>2</sup> ]	Corrosion rate [mmPY]	$I_{corr}$ [A/cm <sup>2</sup> ]	Corrosion rate [mmPY]
Fe <sub>65</sub> Cr <sub>18</sub> Ni <sub>12</sub> Mo <sub>2</sub> Mn <sub>2</sub> (316L)	$3.6 \times 10^{-3}$	1.0	$9 \times 10^{-5}$	0.30
Fe <sub>54</sub> Cr <sub>24</sub> Mn <sub>21</sub> Mo <sub>1</sub> N	$1.6 \times 10^{-4}$	1.2	$6.9 \times 10^{-6}$	0.073
Fe <sub>59</sub> Cr <sub>23</sub> Mn <sub>12</sub> Mo <sub>6</sub> N	$1.3 \times 10^{-5}$	0.18	$2.6 \times 10^{-5}$	0.27
Fe <sub>64</sub> Cr <sub>24</sub> Mn <sub>10</sub> Mo <sub>2</sub> N	$5.1 \times 10^{-4}$	2.1	$4.9 \times 10^{-6}$	0.052

In Ringer's solution tests, the corrosion current,  $I_{\text{corr}}$ , in the case of  $\text{Fe}_{59}\text{Cr}_{23}\text{Mn}_{12}\text{Mo}_6\text{N}$  is  $2.6 \times 10^{-5}$  A/cm<sup>2</sup>. The corresponding values of  $\text{Fe}_{54}\text{Cr}_{24}\text{Mn}_{21}\text{Mo}_1\text{N}$  and  $\text{Fe}_{64}\text{Cr}_{24}\text{Mn}_{10}\text{Mo}_2\text{N}$  are  $6.9 \times 10^{-6}$  and  $4.9 \times 10^{-6}$  A/cm<sup>2</sup>, respectively. Calculated corrosion rates for  $\text{Fe}_{54}\text{Cr}_{24}\text{Mn}_{21}\text{Mo}_1\text{N}$  and  $\text{Fe}_{64}\text{Cr}_{24}\text{Mn}_{10}\text{Mo}_2\text{N}$  steels, 0.073 and 0.052 mmPY, respectively, show that corrosion rate is four times lower than in 316L stainless steel.

Comparison of results obtained for samples in  $\text{H}_2\text{SO}_4$  and Ringer's solution show that synthesized stainless steels manage much better in chloride ions environment. Chemical composition of steels plays bigger role in case of  $\text{H}_2\text{SO}_4$  while in Ringer's solution differences are much smaller.

#### 4. Conclusion

A nanoscale austenitic nickel-free nitrogen containing stainless steel samples were produced by means of the mechanical alloying process and nitrogen absorption. Microhardness test showed that obtained material exhibits Vickers microhardness as high as 520 HV, which is more than two times higher than that of a conventional austenitic stainless steels, including widely used in medicine 316L stainless steel. This is due to the structure refinement and the transformation into nanostructured material, achieved by mechanical alloying method. Such high microhardness did not imply embrittlement of the samples which was proven in 30 kg load test.

Decreasing the corrosion current density is a distinct advantage for prevention of ion release. Nitrogen absorption treatment contributes to the higher corrosion resistance, in both  $\text{H}_2\text{SO}_4$  and Ringer's solution. With regard to austenitic stainless steels it could help to obtain better biomedical implants (e.g. stents) with better mechanical properties, corrosion resistance and biocompatibility.

#### REFERENCES

- [1] I. A. L. Lim, MURJ **11**, 34 (2004).
- [2] IARC Monographs on the Evaluation of Carcinogenic Risks to Humans: Surgical Implants and Other Foreign Bodies, Lyon, **74**, 65 (1999).
- [3] J. Uggowitzer, R. Magdowski, M. Speidel, ISIJ Int. **36**, 901 (1996).
- [4] C. Ornhagen, J. O. Nilsson, H. Vannevik, J. Biomed. Mater. Res. **31**, 97 (1996).
- [5] M. Sumita et al., Materials Science and Engineering C **24**, 753 (2004). bibitem6 H. Gleiter, Prog. Mater. Sci. **33**, 323 (1989).
- [6] M. Tulinski, K. Jurczyk, M. Jurczyk, Inż. Materiałowa **28**, 228 (2007).
- [7] M. Tulinski, K. Jurczyk, M. Jurczyk, Materials Science Poland **26**, 2, 381 (2008). bibitem9 K. Niihara, R. Morena, D. P. H. Hasselmann, J. Mater. Sci. Letters **1**, 13 (1982).